NACA TN 3687

NATIONAL ADVISORY COMMITTEE FOR AERONAUTICS

TECHNICAL NOTE 3687

SOME WIND-TUNNEL EXPERIMENTS ON SINGLE-DEGREE-OF-FREEDOM FLUTTER OF AILERONS IN THE HIGH SUBSONIC SPEED RANGE

By Sherman A. Clevenson

Langley Aeronautical Laboratory
Langley Field, Va.

Washington
June 1956

NATIONAL ADVISORY COMMITTEE FOR AERONAUTICS

TECHNICAL NOTE 3687

SOME WIND-TUNNEL EXPERIMENTS ON SINGLE-DEGREE-OF-FREEDOM FLUTTER OF AILERONS IN THE HIGH SUBSONIC SPEED RANGE[1]

By Sherman A. Clevenson

SUMMARY

Results of wind-tunnel tests of three wing models with various aileron configurations are presented. Density in the range of 0.08×10^{-2} to 0.58×10^{-2} slug per cubic foot has little effect on the initial amplitude or initial Mach number associated with the aileron oscillations (buzz). However, the frequencies decrease somewhat with decrease in density. The initial Mach number associated with buzz decreases with increasing angle of attack, whereas mass balancing and changes in spring stiffness in these tests have little effect. Increasing the aileron mass moment of inertia lowers the oscillation frequency. Placing the aileron at the wing tip delays the onset of buzz to a higher Mach number. There are experimental indications that the buzz range is limited to a range of Mach numbers above the wing critical Mach number. A comparison of the results of the test data with two previously published empirical analyses is made.

INTRODUCTION

Great interest has been shown in wing flutter which essentially involves a single-degree-of-freedom flutter of ailerons on wings of high-speed airplanes (ref. 1). This vibratory instability will be called buzz in this paper. Some buzz tests have been conducted at the Ames Aeronautical Laboratory in the 16-foot wind tunnel (refs. 2 and 3). These tests were made with a full-scale partial-span wing and were limited to one density condition. By use of the facilities of the $4\frac{1}{2}$-foot flutter research tunnel of the Langley Aeronautical Laboratory, it was possible to study effects of the density of the testing medium on this oscillation phenomenon and thus to determine some effects of altitude. In addition, information was obtained on the effects of changes in the inertia and spring stiffness of the aileron, of mass balancing, of angle of attack, and of spanwise aileron location (or tip-relief effect).

---

[1]Supersedes declassified NACA Research Memorandum L9B08 by Sherman A. Clevenson, 1949.

This paper presents the results of the analysis of the data obtained from three wing models with various aileron configurations. It also gives a comparison of the experimental results with the empirical analyses of references 3 and 4.

SYMBOLS

κ_{std}	mass-density parameter at standard air conditions, ratio of a mass of testing medium of diameter equal to chord of wing to mass of wing, both taken for an equal length of span
r_α^2	square of nondimensional radius of gyration of wing about its elastic axis
a	nondimensional coordinate of axis of rotation from midchord
x_α	location of center of gravity measured from a
r_β^2	square of reduced radius of gyration of aileron referred to c
x_β	reduced location of center of gravity of aileron referred to c
c	coordinate of aileron hinge axis
I_β	polar moment of inertia of aileron about its hinge line, slug-ft^2 per foot span
g_h, g_α, g_β	structural damping coefficients
f_{h_1}	first bending natural frequency of wing, cps
f_α	uncoupled first torsion frequency of wing relative to elastic axis, cps
f_β	natural frequency of aileron about its hinge line, cps
f_{init}	experimental frequency of aileron at onset of buzz, cps
k	spring constant of aileron hinges, ft-lb/radian

M	Mach number
M_{cr}	theoretical Mach number at which sonic velocity is first attained on section of wing at zero lift
M_{ch}	experimental Mach number at which wind tunnel chokes
M_{init}	experimental Mach number at which buzz is first observed
A_g	aspect ratio of one wing panel
α	wing angle of attack, deg
ρ	density of test medium, slugs/cu ft

The following sketch taken from reference 5 shows the physical significance of the nondimensional parameters tabulated in table I.

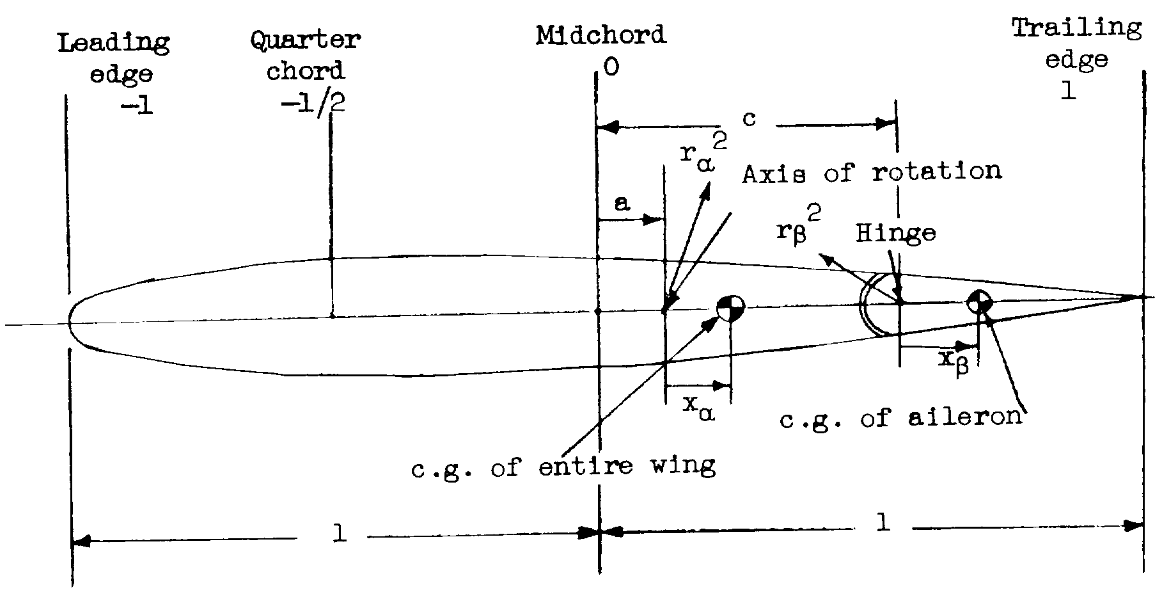

APPARATUS AND METHOD

Models

For this investigation three basic wing forms were used: wing 1, NACA 66,2-215 section; wing 2, 23015 section; and wing 3, 16-016 section.

Because the purpose of the investigation was to study the buzz phenomenon, these wings were made of convenient materials of sufficient stiffness to eliminate other types of flutter. Wing 1 was constructed of bismuth-tin alloy with a dural insert (fig. 1). On its lower surface at aileron midspan were three pressure orifices at 35, 50, and 65 percent wing chord which were connected to three pressure cells. Provision was made to add a spanwise extension at the wing tip (wings 1B and 1C). Figure 2 shows the wing mounted in the tunnel with this spanwise addition. Wing 1A was the basic configuration with or without tufts on its upper and lower surfaces. Wing 2 was of dural construction having the same plan form as wing 1, but with different airfoil section. Wing 3 (fig. 3) was of dural construction and had a smaller chord and larger span than wings 1 and 2. The ailerons were of spruce or balsa construction (with spanwise laminations) with dural blocks at the ends for mounting (fig. 4). For the purpose of mass balancing for some tests, the leading edges of the ailerons were cut away and replaced with bismuth-tin alloy. All aileron chords were 20 percent of the wing chords. These ailerons were mounted to the wings with steel spring hinges (fig. 4). Some tests were also made on a fourth wing, constructed wholly of spruce with a pin-hinged aileron. Wing 4 had an NACA 65-009 section, 12-inch chord, $17\frac{1}{2}$-inch span with a 6-inch aileron span located 2 inches inboard of the wing tip. A list of the wing parameters is presented in table I.

Tunnel

The tests were conducted in the Langley $4\frac{1}{2}$-foot flutter research tunnel which is of the closed-throat single-return type employing air or Freon-12 (having a sound speed of 510 ft per sec at 15° C) at pressures varying from 4 inches to 30 inches mercury absolute. The experimental choking Mach numbers M_{ch} for the wings were as follows: for wing 1A, 0.851; for wings 1B and 1C, 0.831; for wing 2, 0.853; for wing 3, 0.816; and for wing 4, 0.917. Reynolds numbers could be varied from 1×10^{6} to 13×10^{6}. In all cases, the test wing was mounted in a rigid base as a cantilever beam from the top of the tunnel (fig. 2).

Instrumentation

All wing models had bending and torsion strain gages near their bases. For measuring aileron deflection, wings 1, 2, and 3 had strain gages on each hinge of each aileron. Wing 4 had a type of induction position indicator attached to its aileron.

Wing 1 had three dynamic electrical pressure cells connected to three orifices in the wing. Wing 2 had within it an electromagnetic eddy-current damper for the aileron (similar in principle to the standard watt-hour meter). All strain-gage circuits, pressure cells, and position indicators were connected to amplifiers and a carrier system. The electrical impulses were recorded on a 14 channel recording oscillograph.

For visual observations of shock formations and shock waves, a shadowgraph system employing a 100-watt point-source light was utilized. The tunnel test section was painted black except for the top which was painted white. The light source was below the model and directed along the wing span toward the top of the tunnel.

RESULTS AND DISCUSSION

Experimental data are presented in table II and also in figures 5 to 12.

The effect of density on the onset of the oscillation is given in figures 5 and 6. It can be seen that buzz starts with relatively small amplitude (approximately 2° total displacement). The initial Mach number is relatively independent of density. Wings 1A and 1B have essentially constant frequency, but there is seen a tendency for a decrease in frequency with decrease in density. Wings 2 and 3 show a more definite decrease of frequency for decreasing density. A small decrease of frequency with density has been predicted in reference 4. In figure 5, an indication of the tip relief effect is given. There is a definite indication that the Mach number associated with the initiation of buzz with the aileron near the wing tip (wing 1A) is higher than the initial Mach number of the wing with the aileron inboard (wing 1B). The higher Mach number attained is probably due to the higher critical Mach number in the neighborhood of the aileron due to wing tip relief. This result is in accord with the experimental trends presented in reference 3.

Figure 6 gives the data for wing 2, which it may be recalled has an NACA 23015 section. Comparison of these results with those in figure 5 (those referring to wing 2 with similar plan form but with an NACA 66,2-215 section) shows that buzz occurs on the 23015 section at a higher Mach number. This is apparently a wing shape effect. Figure 6 also shows that the buzz frequency may possibly be a range of frequencies at least for this case. However, this rapid change in frequency may be caused by instabilities of flow in the tunnel near tunnel choking

Mach number or by large nonlinear flow effects. Figure 7 is a sample oscillograph record of wing 2 showing the frequency variation from 87 through 107 cycles per second in less than 0.3 seconds of time.

Figure 8 (wing 3, 16-016 section, 8-inch chord) shows that for a constant density condition, the aileron buzz frequency and amplitude increase with an increase in Mach number. For this case, a range of oscillations was obtained. At a Mach number of 0.81, there were indications that the shock position was on the rear part of the aileron and the oscillation stopped abruptly. Even though this phenomenon occurred close to tunnel choking Mach number, this would indicate that buzz occurs in a range of Mach numbers. This is in agreement with statements in references 2 and 4.

The angle of attack was varied on wing 1A, and the results plotted in figure 9. It is seen that the Mach number associated with initial buzz drops off with increasing angle of attack. As indicated by the two sets of data points in figure 9, the low amplitude nonperiodic oscillatory motion appears to precede a larger amplitude sinusoidal motion of the aileron.

Small changes of aileron natural frequency had no appreciable effect on buzz characteristics. Changing the spring constant of the aileron hinge did not affect the frequency of oscillations (fig. 10) obtained previously. The effect of changing the moment of inertia of the aileron is indicated in figure 11. There can be seen a tendency for buzz frequency to decrease with increasing aileron moment of inertia. This is also shown in figure 9(a) of reference 4. In the course of testing, it was determined that mass balancing had little effect on the frequency or initial Mach number of buzz.

By observing initial formation of the shock waves on all the wings tested in Freon-12, it was noted that buzz consistently occurred shortly after a shock wave could be seen. The use of tufts on the wings made it possible to observe the flow separation at approximately the shock-wave position. The rapid oscillation of the shock position could be seen as a blur. The pressure oscillations could be recorded by using dynamic pressure cells or pickups for wing 1. However, due to the time lag of pressure propagation from the wing orifice to the pressure cell, no exact relationship could be determined between the aileron displacement and the position of the shock wave.

Pressure variations at the 35-, 50-, and 65-percent-chord stations were recorded by using dynamic electrical pressure pickups. Figure 12 is a reproduction of the oscillograph record of the pressure oscillation of wing 1C (with a balsa aileron). This pressure variation is approximately 49 pounds per square foot and occurs at a frequency of 85 cycles per second at the 65 percent station for $M = 0.805$. The aileron oscillation occurs at the same frequency. The other two pressure pickups show relatively small pressure variations. Visual observations placed the shock wave at approximately the 65-percent-chord station.

The electromagnetic damper installed in wing 2 gave no positive results. At zero airspeed, the maximum damping, when applied, was 0.00041 foot-pounds per radian per second. During buzz, this amount of damping (equivalent to approximately five times that of the original system) had no effect in changing either the frequency or the magnitude of the oscillation.

An attempt was made to obtain buzz with a relatively thin airfoil. Consequently, wing 4 (NACA 65-009) was used. However, for a density condition of $\rho = 0.0034$ with an unbalanced aileron on wing 4, wing-aileron flutter developed at $M = 0.488$. With a balanced aileron on wing 4, wing bending-torsion flutter developed at $M = 0.895$. Thus, no buzz data were obtained with this wing.

An empirical method of determining buzz frequencies is presented in reference 2 and an example of this method is given in appendix A. The method utilizes an aerodynamic frequency parameter which is then modified in some systematic manner to determine a buzz frequency. The aerodynamic frequencies for wings 1B, 2, and 3 were respectively 112, 75, and 94 cycles per second from which the buzz frequencies were determined to be 56, 38, and 48 cycles per second. These frequencies were based on the velocity of sound in the testing medium, Freon-12. If these frequencies were determined by using the speed of sound in air instead of the velocity of sound in Freon-12, the aerodynamic frequencies would be 220 and 145 for wings 1B and 2, and the corresponding buzz frequencies would be 110 and 74. Reference to table III shows that this empirical method is in better agreement with the experimental results for air than for Freon-12. In this same reference, a criterion was suggested for the prevention of buzz, namely, a sufficiently high aileron moment of inertia to make the aileron natural frequency less than one-half the aerodynamic frequency. For the wing-aileron combinations tested, this criterion was apparently satisfied by a large margin and yet did not prevent buzz.

In reference 4, a hysteresis mechanism is suggested to determine buzz frequency, Mach number and the amount of damping necessary to prevent buzz. The procedure used is to assume the damping and restoring aerodynamic forces and moments lag the velocities and displacements, in particular, because of flow separation. It was found by the use of this analysis (see example in appendix B) that the ailerons of wings 1B, 2, and 3 should have exhibited buzz respectively in a range of Mach numbers of 0.71 through 0.85, 0.70 to 0.81, and 0.71 to 0.82;

at ranges of buzz frequencies respectively of 44 to 70, 23 to 78, and 39 to 55 cycles per second (for a tunnel density of 0.00209 slug per cubic foot). The analysis also showed that it would take damping for the three wings mentioned respectively equivalent to 0.0095 to 0.0126, 0.0154 to 0, and 0.00472 to 0 pound-feet per radian per second per foot span to prevent the oscillation. The damping inherent in the hinges of the ailerons of these three wing combinations were respectively 7.702×10^{-5}, 8.44×10^{-5} (41.0×10^{-5} with the eddy-current damper in operation) and 6.15×10^{-5} pound-feet per radian per second per foot span. The ailerons of these three wings did oscillate but at substantially higher frequencies (see table III) than those predicted, namely in the ranges of 65 to 110, 55 to 130, and 70 to 115 cycles per second, respectively. The corresponding Mach number ranges were 0.72 to 0.851, 0.80 to 0.853, and 0.75 to 0.81. The frequency test data were obtained by using Freon-12 as the testing medium. In order to obtain further insight on the phenomenon, two runs were made with air as the testing medium. For wing 2, approximately the same frequencies and Mach numbers were obtained in air as were obtained by using Freon-12 at the same density. However, for wing 1B the frequency was considerably higher (table III). By applying the analysis of reference 4 to the data points in air, it was seen that the analysis predicted the oscillation at the same Mach numbers with a slightly higher frequency than that predicted previously (table III). Unfortunately the experiments were not as clear cut as one would like them to be, and the separation phenomena in air and Freon-12 were not fully investigated. Thus, although this analysis predicts buzz just above wing critical Mach number and at lower frequencies than those obtained experimentally, it is not wholly inconsistent with the experimental results of these tests. An over-all comparison is found in table III.

CONCLUDING REMARKS

Results presented for these wings show that density of the testing medium in the range of 0.08×10^{-2} to 0.58×10^{-2} slug per cubic foot has little effect on the initial magnitude and initial Mach number of buzz. The buzz frequency decreases somewhat with decrease in density.

The Mach number corresponding to the initial buzz decreases as the wing angle of attack is increased.

Mass balancing the aileron apparently had no effect on buzz; whereas increasing the aileron mass moment of inertia tended to lower the oscillation frequency. Changes of the spring stiffness of the aileron hinges in these tests had no effect on buzz. Placing the aileron at the wing tip delays buzz to a higher Mach number.

There was an indication that a sufficient increase in Mach number to bring the shock-wave position to the rear part of the aileron damps out the buzz; this implies that buzz exists only in a range of Mach numbers above the wing critical Mach number.

A comparison of the experimental results was made with empirical analyses of two references. This comparison showed only qualitative agreement. Refinements both in analysis and experimentation are desirable.

Langley Aeronautical Laboratory,
National Advisory Committee for Aeronautics,
Langley Field, Va., February 10, 1949.

APPENDIX A

EXAMPLE OF THE EMPIRICAL METHOD OF DETERMINING BUZZ FREQUENCY FROM REFERENCE 2

This method assumed that flutter with one degree of freedom can result from a time lag in the changes of flow about a wing. This time is determined as

$$t = \frac{K2d}{a(1 - M)}$$

where

t	time
d	distance from trailing edge to shock
M	free-stream Mach number
a	velocity of sound
K	factor to account for any additional time and estimated to equal 2

By inverting t, a frequency is determined as follows:

$$f_a = \frac{a(1 - M)}{4d}$$

where

f_a	aerodynamic frequency

The phase difference is determined as follows:

$$\phi' = \left(1 - \frac{f}{f_a}\right)360$$

where

ϕ' phase difference between hinge moment and aileron position

f single degree of freedom flutter frequency

The predicted condition for preventing steady flutter is

$$\left[(C\omega)^2 + \left(K_m - I\omega^2\right)^2\right]^{1/2} > A$$

where

C damping coefficient $\left(C_{cr} \frac{g_\beta}{2}\right)$

K_m equivalent spring constant $\left(I\omega_o^{\,2}\right)$

I mass moment of inertia of the aileron

A variation of the hinge moment with aileron angle

$\omega = 2\pi f$

$$\tan \phi' = \frac{C\omega}{K_m - I\omega^2}$$

Since $\phi' = \left(1 - \frac{f}{f_a}\right)360$, the determination of f is

$$\frac{\omega}{2\pi} = f = \frac{f_a}{360}\left[-\tan^{-1}\left(\frac{C\omega}{K_m - I\omega^2}\right) + 360\right]$$

If K_m is smaller than $I\omega^2$, f is between $0.5f_a$ and $0.75f_a$, and when K_m is greater than $I\omega^2$, f is between $0.75f_a$ and f_a.

By applying the parameters of wing 1A,

$$f_a = \frac{a(1 - M)}{4d} = \frac{510(1 - 0.71)}{4 \times 0.333} = 112 \text{ cps}$$

$$K_m = I\omega_o^2 = 12 \times 2.339 \times 10^{-5} \frac{10}{12}(2\pi 10.5)^2 = 1.018$$

$$C_{cr} = 2\sqrt{K_m I}$$

$$\frac{g_\beta}{2} = \frac{0.05}{2} = 0.025$$

$$C = 0.025C_r = 0.025 \times 2 \sqrt{1.018 \times 2.339 \times 10^{-4}}$$

$$C = 0.05 \times 0.0154 = 0.77 \times 10^{-3}$$

Therefore,

$$\frac{\omega}{2\pi} = f = \frac{112}{360}\left(-\tan^{-1} \frac{0.77 \times 10^{-3}\omega}{1.018 - 2.339 \times 10^{-4}\omega^2} + 360\right)$$

and is solved graphically

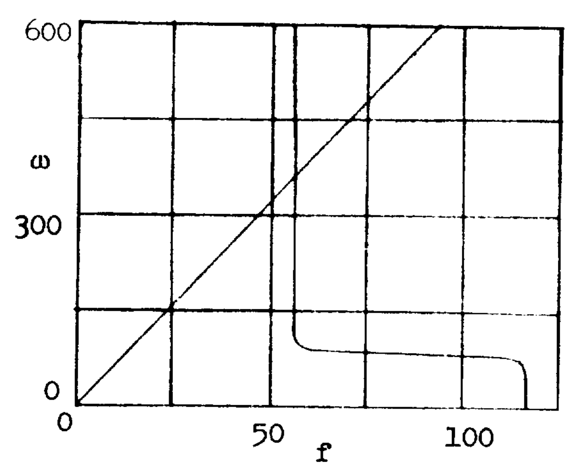

Thus it is seen that the predicted frequency of this single degree of freedom flutter is 56 cycles per second.

APPENDIX B

EXAMPLE OF ANALYTICAL METHOD OF REFERENCE 4

The following example indicated how the data of wing 2 is applied to the analysis of reference 4:

Physical Data

Mach number	0.70
Velocity, feet/second	357
Aileron moment of inertia about hinge line, slug-foot^2 . .	1.92×10^{-5}
Aileron span, feet	0.83
Wing chord at midaileron span, feet	0.83
Density of medium, slug/foot^3	0.00209
Geometric aileron hinge-line location, percent wing chord . .	80
Geometric aileron leading-edge location, percent wing chord	75
Natural frequency of aileron, cycles per second	10.2

Computed Parameters (See reference 6.)

$$b = \frac{0.83}{2} = 0.415$$

$$c = \frac{2 \times 80}{100} - 1 = 0.6$$

$$e = \frac{2 \times 75}{100} - 1 = 0.5$$

$$I_t = I_\beta = 2.3 \times 10^{-5}$$

$$\frac{I}{\pi \rho b^4} = 0.119$$

$$\sqrt{\frac{1}{1 - M^2}} = 1.397$$

$$\omega_o = (10.2)(2\pi) = 64.2 \text{ radians/second}$$

Estimation of Time Lag

$$t = t_a + t_b + t_c + t_d$$

$$t_a = \int_{s_1}^{s_2} \frac{ds}{a - v} = \frac{s_2 - s_1}{a - v}$$

$$t_b = t_a$$

$$t_c = \int_{s_1}^{s_2} \frac{ds}{a - v} = \frac{s_2 - s_1}{a}$$

where v is assumed equal to zero and t_d is assumed to be very small and

s_1 chordwise location of shock wave on airfoil in feet

s_2 chordwise location of some point on aileron (in feet) which can be used as an effective center of pressure

a local speed of sound

v local velocity of the medium

At $M = 0.7$

s_1 = 35-percent chord

s_2 = 83-percent chord

$a - v$ (averaged over the distance $s_2 - s_1$) = 76 fps

$$t_a = \frac{0.83 - 0.35}{76} \frac{10}{12} = 0.00526$$

$$t_b = 0.00526$$

$$t_c = \frac{0.83 - 0.35}{510} \frac{10}{12} = 0.000784$$

$$t = 0.0113$$

By using equation (19) of reference 4

$$\phi = 57.3\omega t$$

Then

$$\phi = 0.647\omega$$

where ϕ is the phase angle during the oscillation by which the actual air-flow circulation lags behind that corresponding to potential flow.

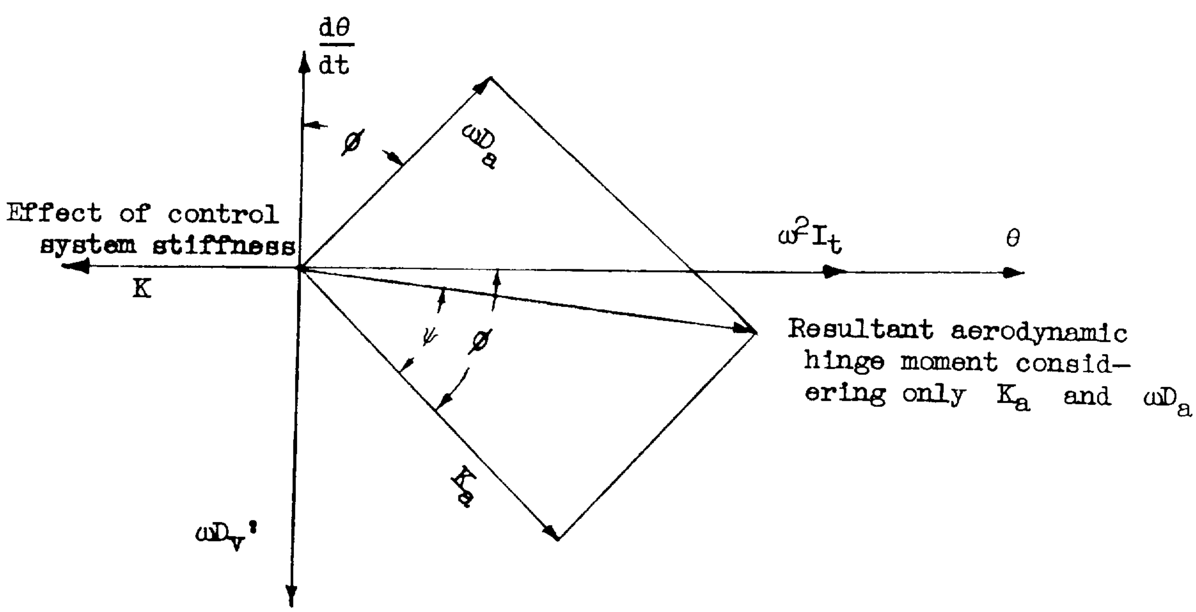

Calculation of Aerodynamic Hinge Moments

The equation of the hinge moments is as follows (terms defined in reference 6):

$$T = \theta_o \pi \rho b^4 \omega^2 \sqrt{\frac{1}{1 - M^2}} \left[T_\beta - (c - e)\left(T_z + P_\beta\right) + P_z(c - e)^2\right]$$

and is dependent on the flutter parameter $v/b\omega$. The real and imaginary components of the moment are computed and in nondimensional form are

$$\text{Real component} = \frac{K_a}{\pi \rho b^4 \omega^2}$$

$$\text{Imaginary component} = \frac{\omega D_a}{\pi \rho b^4 \omega^2}$$

From the geometry of the preceding figure, it can be shown that

$$\cos(\phi - \psi) = \frac{\frac{I_t}{\pi \rho b^4}}{\frac{-K_a}{\pi \rho b^4 \omega^2}} \left[1 - \left(\frac{\omega_o}{\omega}\right)^2\right] \cos \psi$$

from which ϕ can be determined for various values of $v/b\omega$

$\frac{v}{b\omega}$	ϕ_1	ϕ_2	ω
2.50	64	0	336
3.33	84	-38	252
3.75	87	-47	224
10.00	93	-85	84

These values are plotted as ϕ against ω on the same plot as $\phi = 0.647\omega$. The intersection of these curves determines the resultant phase angle and frequency of oscillation as shown in the following figure

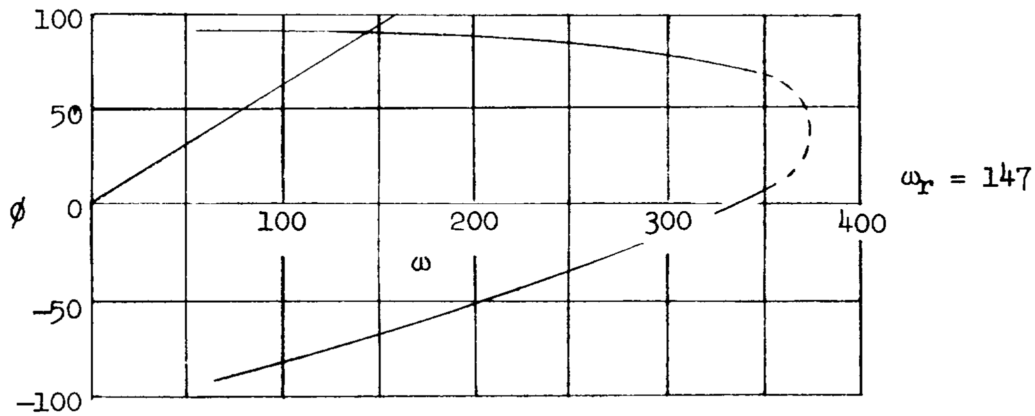

By using the resultant frequency and phase angle in the following equation (also determined from the geometry of fig. under section entitled "Estimation of Time Lag"), the value of damping necessary to prevent the oscillation is determined.

$$\sin(\phi - \psi) = \frac{D_v'}{\pi\rho b^4\omega}\left(\frac{1}{\frac{-\omega Da}{\pi\rho b^4\omega^2}}\right)\sin\psi$$

Thus the predicted frequency of oscillation is 23.4 cycles per second at $M = 0.7$ and would take an amount of damping equivalent to 0.0154 pound-feet per radian per second per foot span of the aileron to prevent the oscillation.

REFERENCES

1. Goethert, Bernhard: Comments on Aileron Oscillations in the Shock-Wave Range. AAF TR No. F-TR-2101-ND, Materiel Command, Army Air Forces, July 1947.

2. Erickson, Albert L., and Stephenson, Jack D.: A Suggested Method of Analyzing for Transonic Flutter of Control Surfaces Based on Available Experimental Evidence. NACA RM A7F30, 1947.

3. Perone, Angelo, and Erickson, Albert L.: Wind-Tunnel Investigation of Transonic Aileron Flutter of a Semispan Wing With an NACA 23013 Section. NACA RM A8D27, 1948.

4. Smilg, Benjamin: The Prevention of Aileron Oscillations at Transonic Airspeeds. AAF TR No. 5530, Materiel Command, Army Air Forces, Dec. 24, 1946.

5. Theodorsen, Theodore, and Garrick, I. E.: Mechanism of Flutter - A Theoretical and Experimental Investigation of the Flutter Problem. NACA Rep. 685, 1940.

6. Smilg, Benjamin, and Wasserman, Lee S.: Application of Three-Dimensional Flutter Theory to Aircraft Structures. ACTR No. 4798, Materiel Div., Army Air Corps, July 9, 1942.

TABLE I

WING AND AILERON PARAMETERS

Wing \ Parameter	$\frac{1}{\kappa_{std}}$	r_α^2	a	x_α	r_β^2	x_β	c	I_β
1A	694	0.230	-0.126	0.033	15.0×10^{-5}	7.75×10^{-3}	0.6	2.339×10^{-5}
1B	550	.230	-.126	.033	18.0	5.65	.6	2.339
1C	550	.230	-.126	.033	7.9	3.40	.6	1.031
2	284	.224	-.140	.000	38.8	3.88	.6	2.300
3	340	.230	-.050	.020	72.0	2.64	.6	2.270
4	28	.210	-.192	.140	112	10.50	.6	1.381

Wing \ Parameter	g_h	g_α	g_β	f_{h_1}	f_α	f_β	M_{cr}	M_{ch}	A_g
1A	0.040	0.050	0.050	12.0	138	10.5	0.71	0.851	2.70
1B	.050	.060	.060	13.6	138	10.5	.71	.831	3.50
1C	.081	.021	.025	13.8	122	13.5	.71	.831	3.50
2	.141	----	.140	47.5	135	10.2	.67	.853	2.70
3	.081	.002	.062	64.0	210	12.2	.71	.816	6.00
4	.050	.100	.000	74.0	123	00.0	.79	.917	1.38

TABLE II

EXPERIMENTAL DATA

α, deg	ρ, slugs/cu ft	Aileron amplitude, deg	M_{init}	f_{init}, cps
Figure 5				
	Wing 1A			
0	0.327×10^{-2}	1.78	0.788	69
	.377	.89	.782	68
	.406	1.78	.756	69
	.426	.89	.757	70
	.530	3.56	.768	69
	.583	1.78	.775	77
	Wing 1B			
0	0.359×10^{-2}	1.78	0.734	68
	.403	2.67	.748	78
	.478	1.78	.760	79
	.560	1.78	.750	80
	Wing 3			
0	0.261×10^{-2}	2.24	0.802	64
	.408	2.24	.770	71
	.485	2.24	.770	84
	.580	3.36	.785	105
Figure 6				
	Wing 2			
0	0.084×10^{-2}	3.56	0.835	48
	.176	3.56	.839	70, 76
	.209	3.56	.839	70–85
	.227	3.56	.836	70–74
	.248	2.67	.834	74–82
	.269	2.67	.835	73–81
	.293	2.67	.837	68–100
	.314	3.56	.812	94–100
	.346	3.56	.833	83–97
	.361	3.56	.835	99–119
	.384	1.78	.833	95–105
	.407	2.67	.831	95–105
	.431	----	.827	------
	.450	1.78	.825	91–104
	.475	3.56	.823	95–100

α, deg	ρ, slugs/cu ft	Aileron amplitude, deg	M_{init}	f_{init}, cps
Figure 8				
Wing 3				
0	0.521×10^{-2}	0	0.759	---
0	.521	2.24	.760	70
0	.521	3.36	.768	91
0	.521	3.36	.777	98
0	.521	4.48	.787	100
0	.521	6.72	.797	106
0	.521	6.72	.807	113
Figure 9				
Wing 1A				
-6	0.261×10^{-2}	0.89	0.769	70
-3	.261	.89	.761	67
0	.261	.89	.744	67
3	.261	.89	.734	69
6	.261	.89	.731	69
9	.261	.89	.683	67
-6	.261	2.67	.800	70
-3	.261	2.67	.795	67
0	.261	2.67	.794	67
3	.261	2.67	.780	69
6	.261	2.67	-----	69
9	.261	2.67	-----	67
k, ft-lb/radian	**ρ, slugs/cu ft**	**I_β, slug-ft^2 per foot span**	**M_{init}**	**f_{init}, cps**
Figures 10 and 11				
0.0283	0.59×10^{-2}	1.03×10^{-5}	0.76	70
.0525	.59	1.03	.76	70
.0625	.59	1.03	.76	69
.0525	.59	1.03	.73	70
.0525	.66	2.34	.76	59
.0525	.54	3.82	.77	57

TABLE III

COMPARISON OF REFERENCE ANALYSES WITH EXPERIMENTAL DATA

Wing	ρ, slugs/cu ft	Reference 4						Reference 2			
		Damping to prevent buzz		Buzz frequency		Buzz Mach number range		Aerodynamic frequency		Buzz frequency	
		Freon	Air	Freon	Air	Freon	Air	Freon	Air	Freon	Air
1B	0.00055	------	0.0036	-----	56-89	---------	0.71-0.85	112	220	56	110
1B	0.00209	0.0095	------	44-70	-----	0.71-0.85	---------	112	220	56	110
2	0.00036	------	0.0052	-----	36-74	---------	0.70-0.84	75	145	38	74
2	0.00210	0.0154	------	23-78	-----	0.70-0.81	---------	75	145	38	74
3	0.00209	0.0047	------	39-55	-----	0.71-0.82	---------	94	182	48	91

Wing	ρ, slugs/cu ft	Experimental data					
		Damping inherent in aileron	Aileron natural frequency	Aileron buzz frequency range		Aileron Mach number range for buzz	
				Freon	Air	Freon	Air
1B	0.00062	0.000077	10.5	54-105	112-125	0.74-0.81	0.67-0.82
1B	0.00209	0.000077	10.5	65-110	-------	0.72-0.85	---------
2	0.00043	0.000084	10.2	47-92	47-67	0.81-0.85	0.77-0.86
2	0.00210	0.000084	10.2	55-130	-------	0.80-0.85	---------
3	0.00209	0.000062	12.2	70-115	-------	0.75-0.81	---------

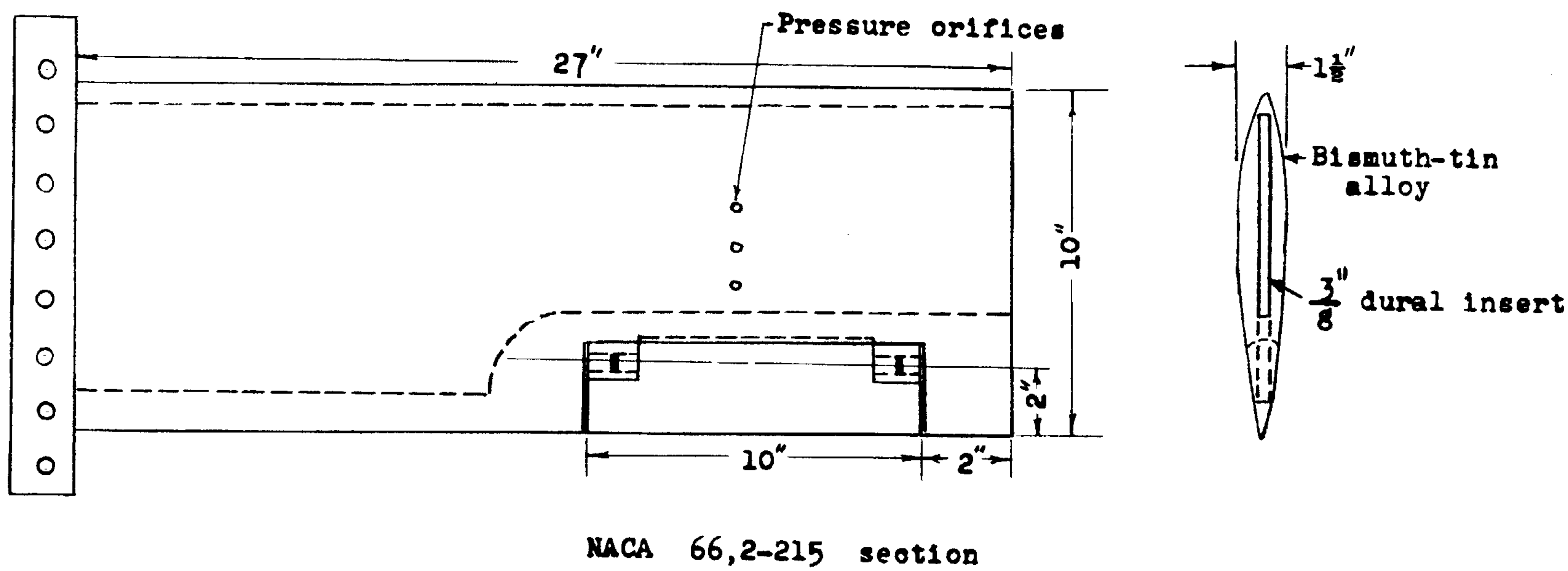

Figure 1.– Sketch of construction and dimensions of wing 1.

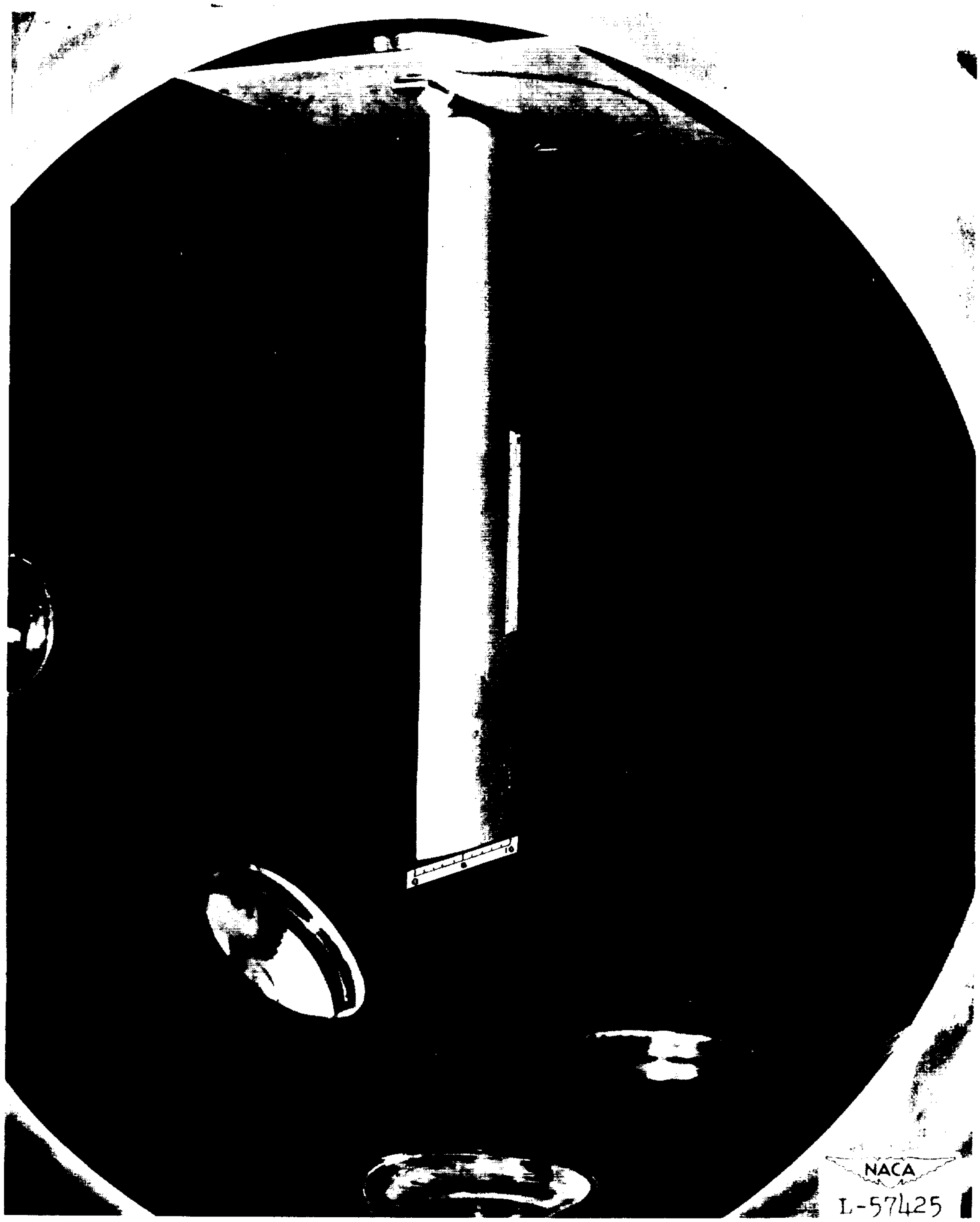

Figure 2.- Model 1C mounted in the Langley $4\frac{1}{2}$-foot flutter research tunnel.

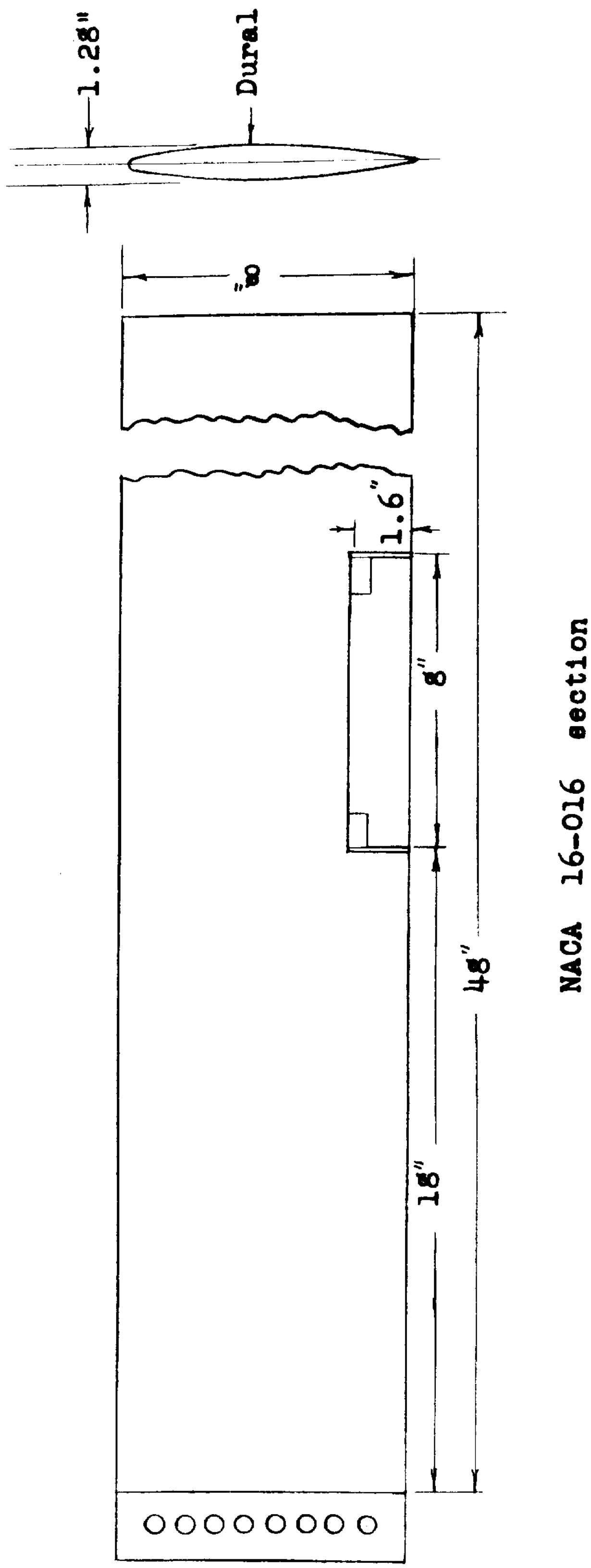

Figure 3.- Sketch of the construction and dimensions of wing 3.

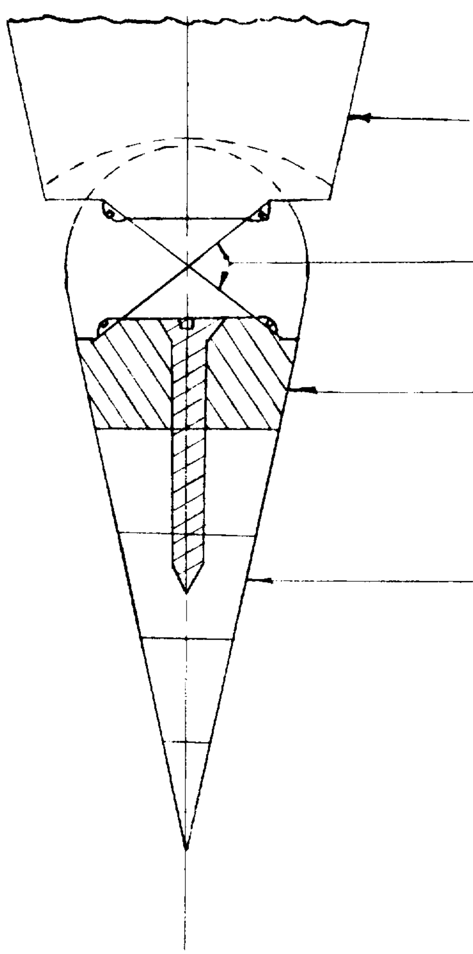

Figure 4.– Diagramatic view showing aileron mounted to wing on steel hinges.

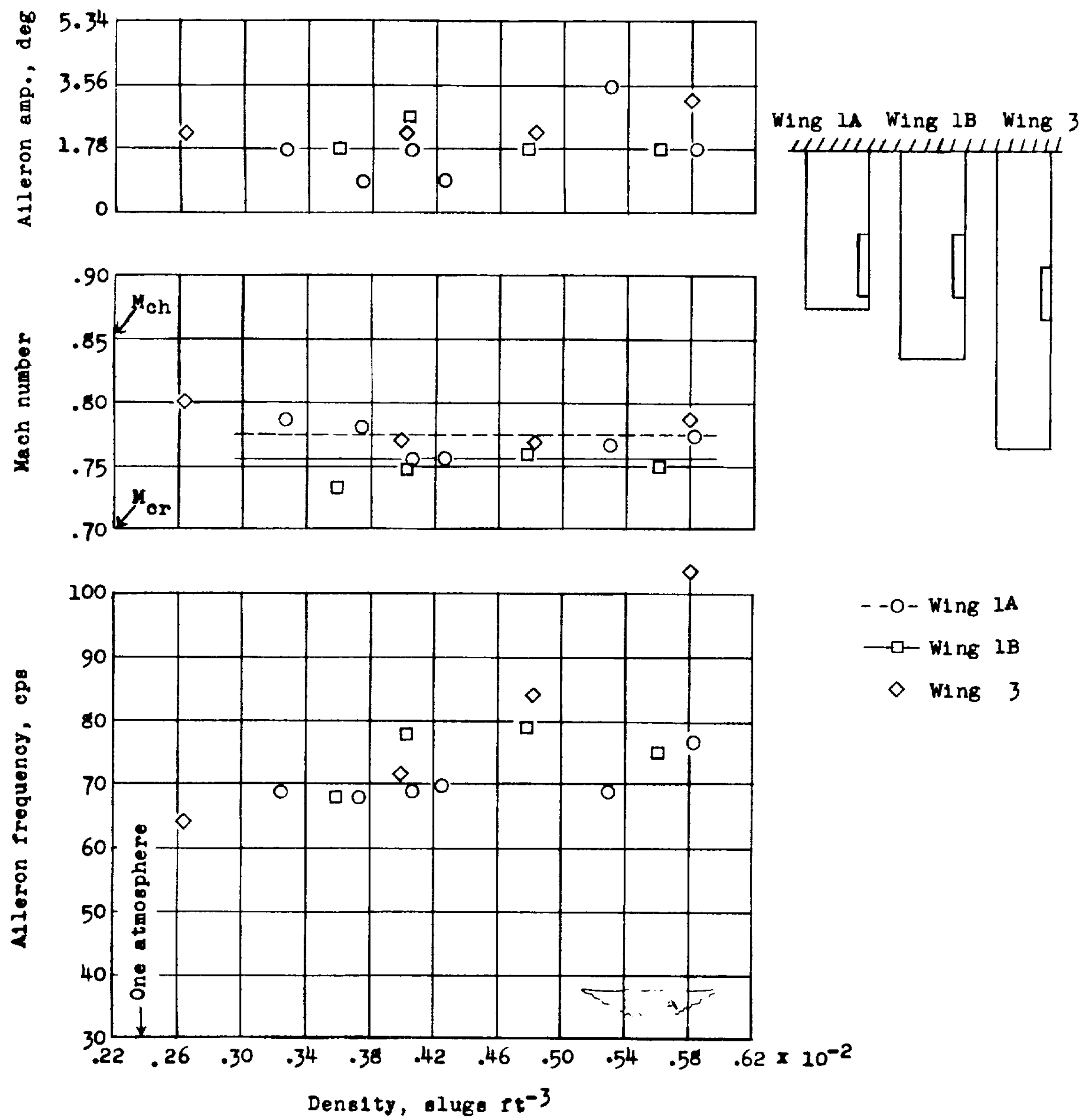

Figure 5.– Aileron frequency, Mach number, and amplitude against density at onset of buzz. Wings 1A, 1B, and 3; $\alpha = 0^{\circ}$.

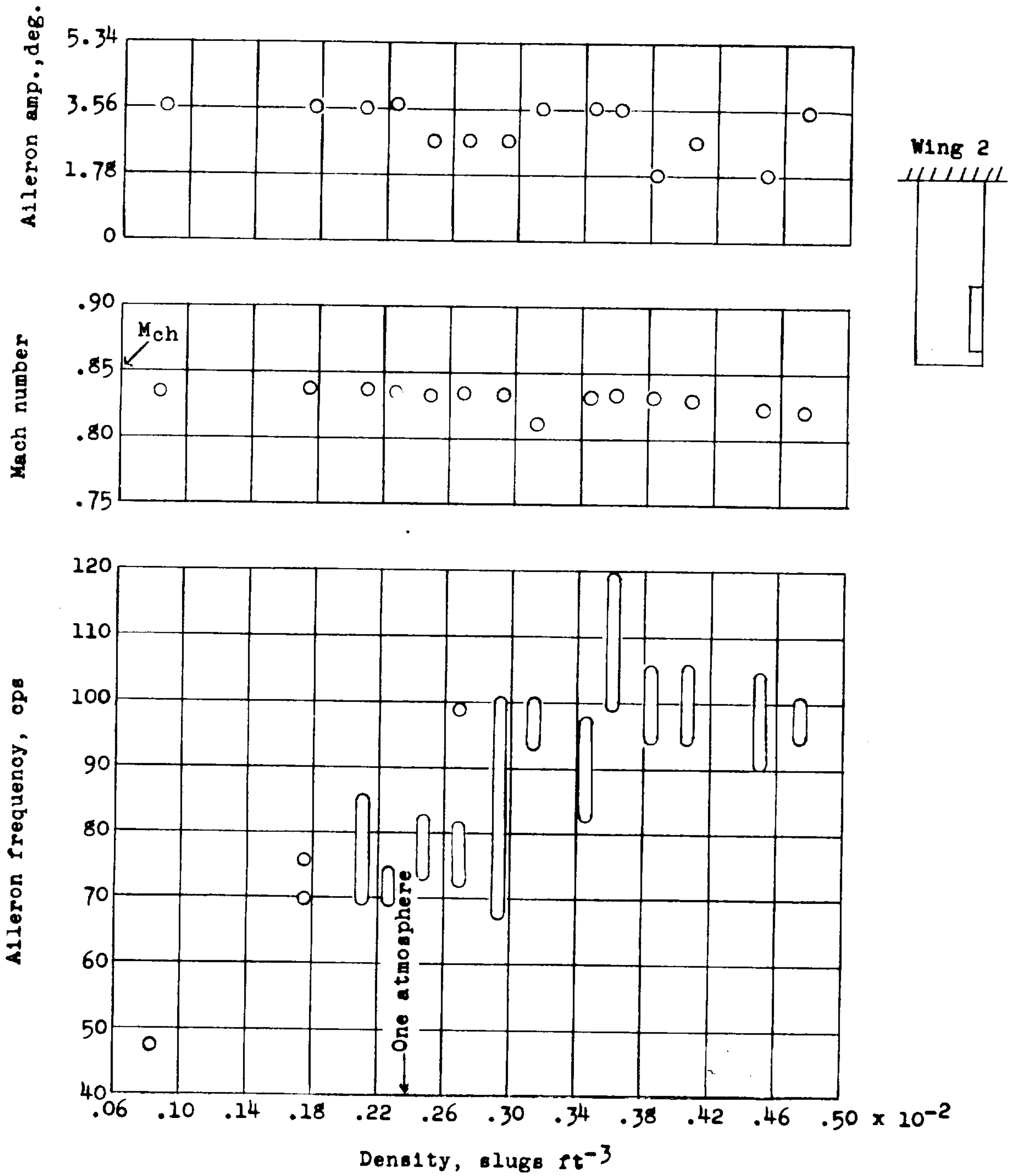

Figure 6.– Aileron frequency, Mach number, and amplitude against density at onset of buzz. Wing 2; $\alpha = 0^{\circ}$.

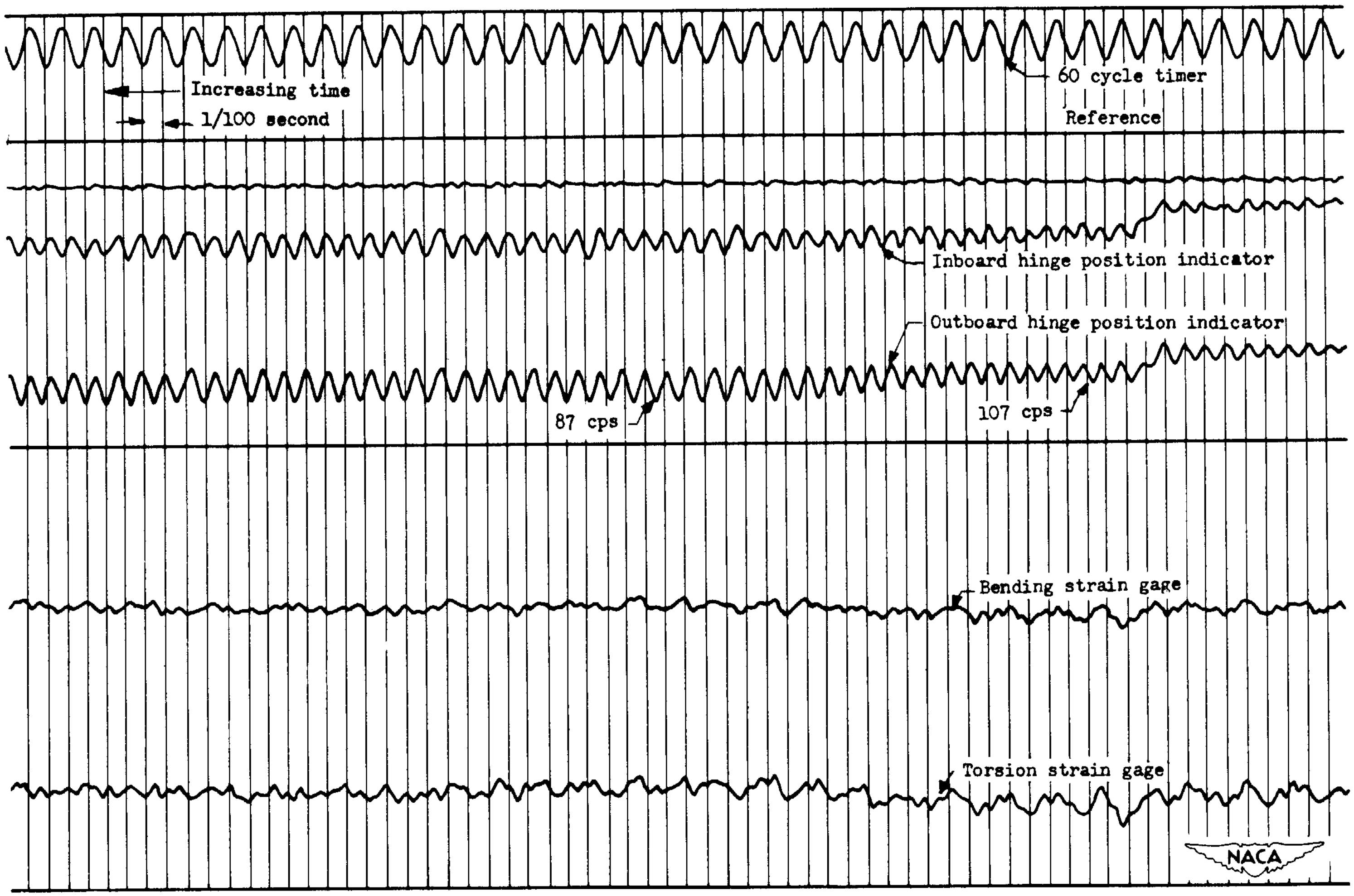

Figure 7.– Aileron variation of buzz frequency at Mach number. $M = 0.833$; wing 2; $\rho = 0.0031$.

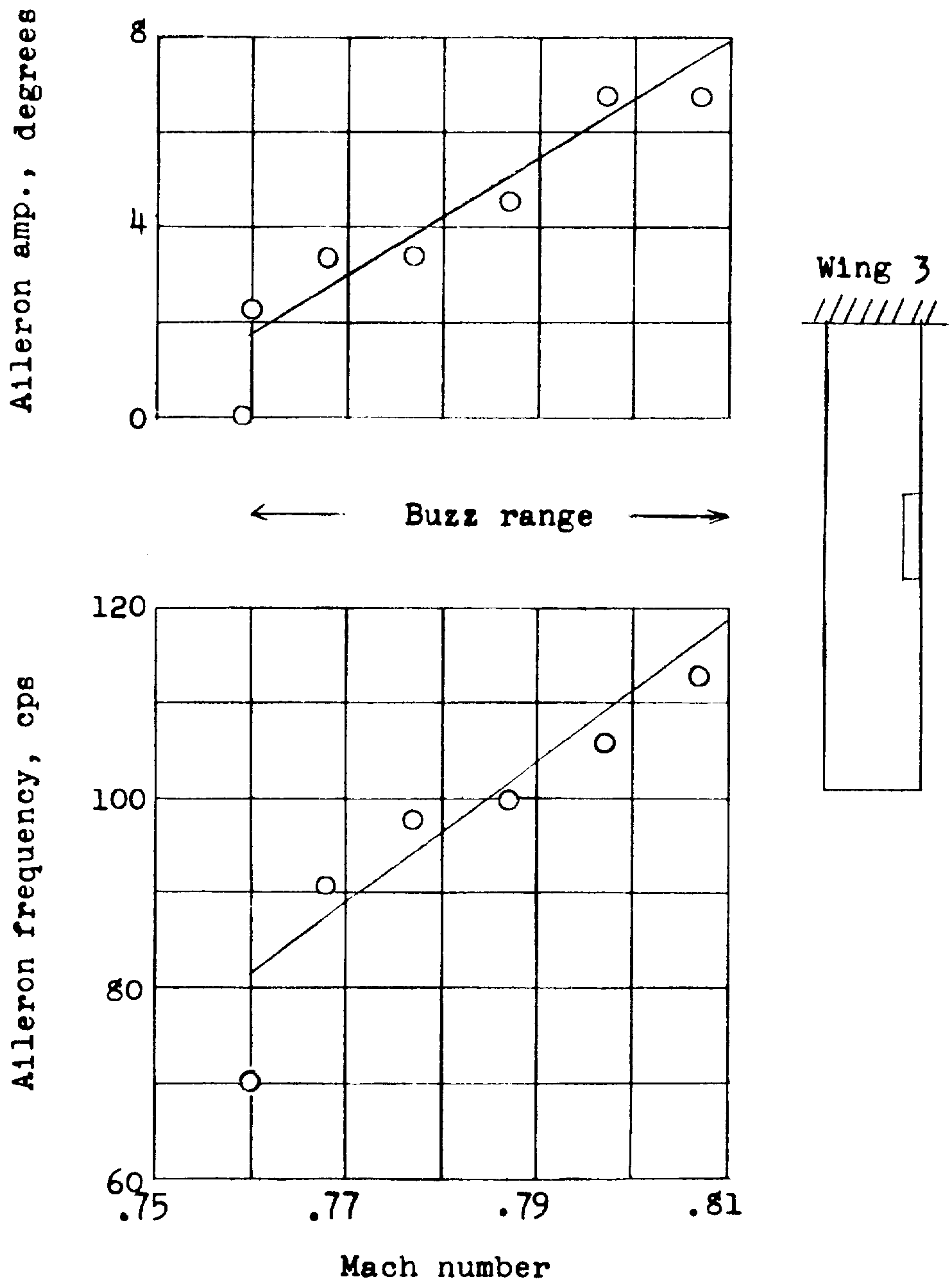

Figure 8.– Aileron frequency and amplitude against Mach number. Wing 3; ρ = 0.00521; α = 0°.

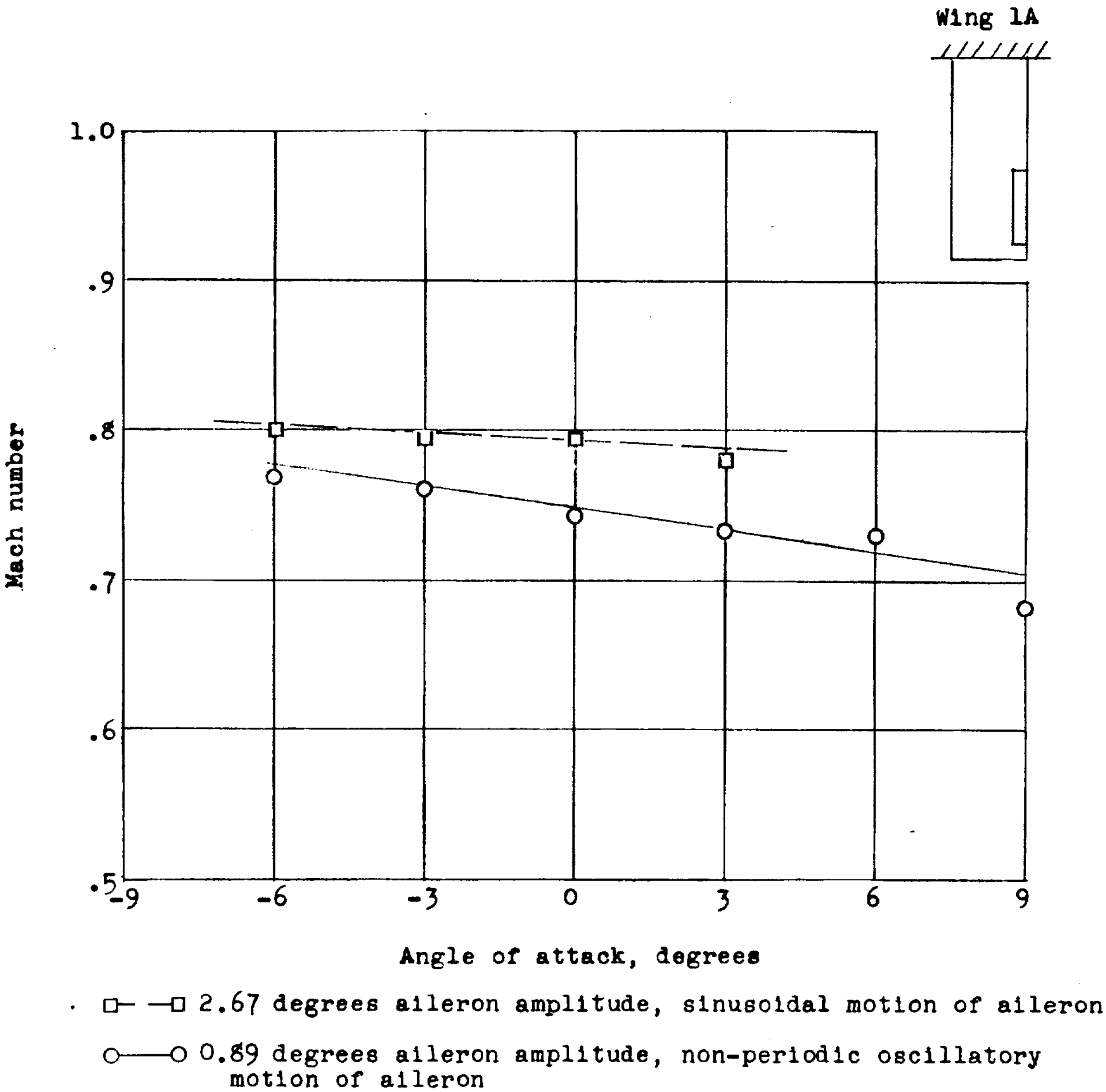

Figure 9.- Buzz Mach number against angle of attack.
Wing 1A; $\rho = 0.00261$.

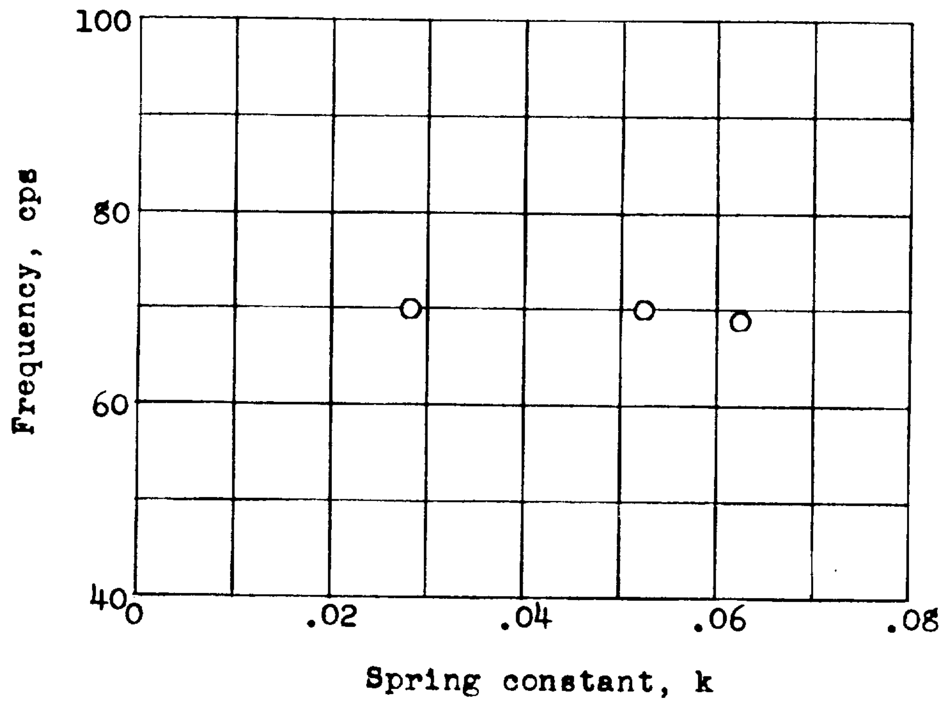

Figure 10.– Aileron buzz frequency against aileron spring constant. Wing 1C; $M = 0.76$; $\rho = 0.00586$ (average); $I_\beta = 1.031 \times 10^{-5}$.

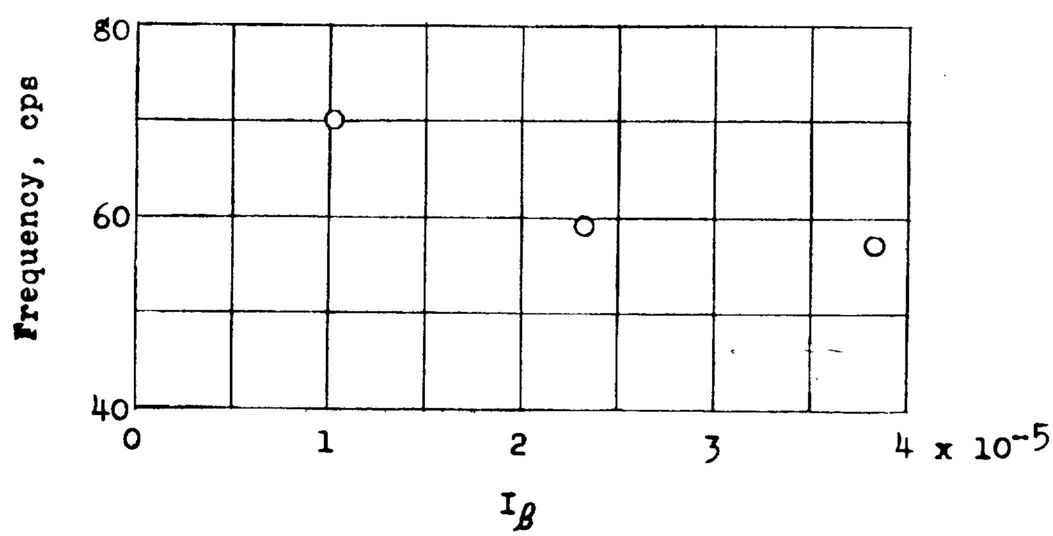

Figure 11.– Aileron buzz frequency against aileron moment of inertia. $M = 0.76$; $\rho = 0.00586$ (average); $k = 0.0525$.

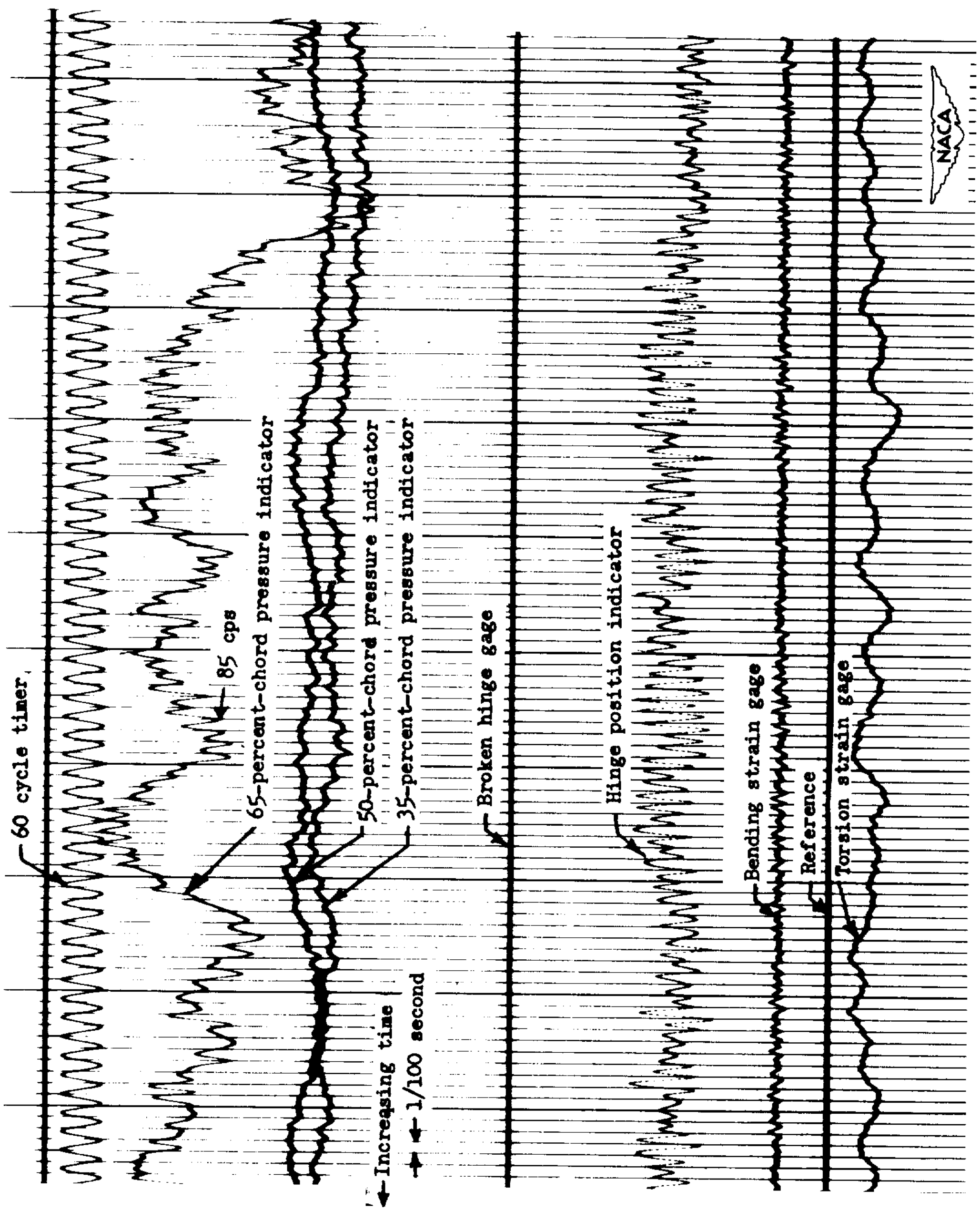

Figure 12.- Pressure oscillations at 65-percent chord. Wing 1A; M = 0.805; ρ = 0.0037.